Stem Cell Reports
Article
ISSCR
OPEN ACCESS

PKM2 is a key factor to regulate neurogenesis and cognition by controlling lactate homeostasis

Pengyan He,[1,8] Bingjun Zhang,[1,8] Wei Jiang,[1] Fan Zhu,[1] Ziqi Liang,[2] Lin Gao,[2] Yuhong Zhang,[3] Yuge Wang,[1,*] Caixia Wu,[4,5,6,*] and Changyong Tang[1,7,9,*]

[1]Department of Neurology, The Third Affiliated Hospital of Sun Yat-Sen University, 600 Tianhe Road, Guangzhou 510630, Guangdong Province, China
[2]State Key Laboratory for Molecular and Developmental Biology, Institute of Genetics and Developmental Biology, Chinese Academy of Sciences, Beijing 100101, China
[3]The Affiliated Brain Hospital, Guangzhou Medical University, Key Laboratory of Neurogenetics and Channelopathies of Guangdong Province and the Ministry of Education of China, Guangzhou Medical University, Guangzhou 510370, China
[4]Institute of Biological and Medical Engineering, Guangdong Academy of Sciences, Guangzhou 510632, China
[5]National Engineering Research Center for Healthcare Devices, Institute of Biological and Medical Engineering, Guangdong Academy of Sciences, Guangzhou 510316, China
[6]Guangdong Provincial Key Laboratory of Medical Electronic Instruments and Polymer Material Products, Institute of Biological and Medical Engineering, Guangdong Academy of Sciences, Guangzhou 510316, China
[7]Guangdong Provincial Key Laboratory of Diabetology, The Third Affiliated Hospital of Sun Yat-sen University, Guangzhou, Guangdong 510630, China
[8]These authors contributed equally
[9]Lead contact
*Correspondence: wangyuge@mail.sysu.edu.cn (Y.W.), caixia52@163.com (C.W.), tangchy23@mail.sysu.edu.cn (C.T.)
https://doi.org/10.1016/j.stemcr.2024.11.011

SUMMARY

Adult hippocampal neurogenesis (AHN), the process of generating new neurons from adult neural stem/progenitor cells (NSPCs), is crucial for cognitive functions and is influenced by numerous factors, including metabolic processes. Pyruvate kinase M2 (PKM2), a key rate-limiting enzyme in glycolysis, catalyzes the production of pyruvate, which undergoes either oxidative phosphorylation or anaerobic oxidation. We observed that PKM2 is highly expressed in NSPCs, but its significance remains unclear for AHN and cognition. Using knockdown or knockout strategies, we discovered that PKM2 deficiency led to reduced AHN and impaired cognitive functions. Furthermore, we observed that knockout of PKM2 resulted in lower L-lactate levels, and supplementing L-lactate in PKM2 knockout mice improved AHN and cognitive functions. Mechanistically, L-lactate restored neurogenesis via monocarboxylate transporter 2 (MCT2), but not hydroxycarboxylic acid receptor 1. In summary, our findings demonstrate that PKM2 is essential for AHN, and lactate supplementation can restore neurogenesis in an MCT2-dependent manner.

INTRODUCTION

Adult neurogenesis, the process of generating functional neurons from adult neural progenitor/stem cells (NSPCs), occurs in two primary neurogenic niches in the adult mammalian brain: the subventricular zone (SVZ) of the lateral ventricles and the subgranular zone (SGZ) within the dentate gyrus (DG) of the hippocampus (Bond et al., 2015). In rodents, adult hippocampal neurogenesis (AHN) is closely linked to cognitive functions. For instance, spatial memory, particularly long-term memory retention in tasks such as the Morris water maze (MWM), has been shown to rely on AHN (Tronel et al., 2012). Additionally, cognitive flexibility, which involves the ability to switch behavioral responses and adopt new strategies, is also associated with AHN, which has been demonstrated in the reverse Morris water maze (RMWM) (Epp et al., 2016).

Over the past decades, extensive research has identified a variety of factors and mechanisms that influence AHN. These include signaling transduction components, transcription factors, and metabolic processes (Gonçalves et al., 2016). Metabolic processes, in particular, have emerged as key regulators of the proliferation and differentiation of NSPCs. Previous research has demonstrated that stem cells typically maintain a distinct metabolic state compared to their differentiated progeny (Folmes et al., 2011). To be specific, it is believed that glycolysis is one of the major metabolic processes in NSPCs that provides substrates for biosynthesis and provides energy to meet the high energy requirement (Ferreira et al., 2018). Pyruvate kinase M (PKM) is a key enzyme in glycolysis, yet whether it has any roles in adult neurogenesis remains elusive.

PKM is a rate-limiting enzyme in glycolysis, catalyzing the step of transferring a phosphate group from phosphoenolpyruvate (PEP) to adenosine diphosphate (ADP), resulting in the production of adenosine triphosphate (ATP) and pyruvate (Zhu et al., 2021). The PKM gene encodes two different isoenzymes, PKM1 and PKM2. PKM1 is predominantly expressed in cells with high catabolic demand, such as muscle cells and neurons, whereas PKM2 is primarily found in proliferating cells, including embryonic cells, tumor cells, and neural progenitor cells of the hippocampus and subventricular region (Romero-Ramírez et al., 2022). It is well established that PKM2 plays a crucial role in tumor development, primarily due to its characteristics

of regulating glycolysis and mediating downstream signaling pathways (Wu et al., 2024). Previous studies have shown that PKM2 increases angiogenesis, neurogenesis, and functional recovery after ischemic stroke (Chen et al., 2018). However, the exact mechanism by which PKM2 regulates AHN under normal physiological conditions remains ambiguous.

Generally, pyruvate either enters the citric acid cycle in the mitochondria under normal physiological conditions or converts to lactate through lactate dehydrogenase (LDH) under conditions of reduced oxygen availability (Valvona et al., 2016). Previous studies have shown that the production of vascular endothelial growth factor (VEGF), a strong inducer of AHN, is mediated by activation of the lactate receptor hydroxycarboxylic acid receptor 1 (HCAR1) (Morland et al., 2017). Moreover, in experimental intracerebral hemorrhage, lactate is found to facilitate angiogenesis and neurogenesis by activating the nuclear factor κB (NF-κB) signaling pathway (Zhou et al., 2018).

Lactate is transported through the membrane via monocarboxylate transporters (MCTs), such as MCT2 and MCT4. MCT2 is mainly expressed on neurons, and MCT4 is expressed on astrocytes (Elizondo-Vega and García-Robles, 2017). Lactate is transferred from astrocytes to neurons through MCT2, and LDH1 converts lactate back to pyruvate in neurons, which is later transported to mitochondria and enters the tricarboxylic acid cycle (TCA) for oxidative phosphorylation (Deitmer et al., 2019). HCAR1, a lactate receptor, is highly expressed in adipose tissue and downregulates the production of cyclic AMP (cAMP) and promotes storage of metabolites (Ahmed et al., 2009). HCAR1 is also expressed in the brain, including in the principal neurons in the cerebral cortex, cerebellum, and hippocampus (Lauritzen et al., 2014). Apart from facilitating the production of VEGF mentioned before, HCAR1-related activation of lactate may be connected with synaptic plasticity and energy metabolism (Bergersen, 2015).

Considering the fact that PKM2 plays an indispensable role in energy metabolism, we hypothesized that PKM2 is also necessary for AHN. Thus, we ablated PKM2 in NSPCs both *in vitro* and *in vivo* and validated that with PKM2 deficiency, NSPC proliferation and differentiation were compromised. Meanwhile, impaired cognitive functions such as spatial memory and cognitive flexibility were shown in PKM2-deficient mice. Furthermore, lactate supplementation was proven to counteract the negative effects of PKM2 deficiency, elevating AHN and improving behavioral performances. Additionally, we determined that lactate exerts its effect of restoring AHN in PKM2-deficient conditions via MCT2. Collectively, our data demonstrate that PKM2 is critical for AHN and lactate supplementation can restore neurogenesis in an MCT2-dependent manner.

RESULTS

PKM2 deficiency leads to compromised AHN

PKM2, a pivotal rate-limiting enzyme in glycolysis, is primarily expressed in proliferating cells, notably in embryonic cells, the cerebellum, neural progenitor cells of the hippocampus, and the subventricular region (Romero-Ramírez et al., 2022). To elucidate the function of PKM2 in NSPCs, we initially conducted immunofluorescence staining to assess PKM2 expression in the hippocampus of adult mouse brains. Our immunostaining analysis confirmed abundant PKM2 expression in glial fibrillary acidic protein ($GFAP^+$)$Sox2^+$ radial glial-like (RGL) cells and $GFAP^-Sox2^+$ progenitor cells (Figures 1A and 1B), with a lesser presence in DCX^+ (doublecortin) immature neurons (Figure 1C) and an absence in $NeuN^+$ mature neurons (Figure S1A), indicating a decline in expression during differentiation (Figures 1D and S1B).

To investigate whether PKM2 is crucial for NSPC proliferation and differentiation, we utilized a lentivirus expressing PKM2 short hairpin RNA (shRNA) and red fluorescent protein (RFP) to reduce PKM2 expression *in vitro* (Figure S1C). Primary mouse NSPCs were isolated and cultured from the DG of young adult mice and then infected with shPKM2 or shNC (negative control) lentivirus. Western blot analysis revealed a significant reduction in PKM2 protein levels in shPKM2 NSPCs compared to shNC NSPCs, indicating successful transduction and high knockdown efficiency (Figure S1D). Immunofluorescence analysis demonstrated a notable decrease in EdU^+ (5-Ethynyl-2′-deoxyuridine) NSPCs (proliferating cells) in the shPKM2 group, highlighting the importance of PKM2 for NSPC proliferation *in vitro* (Figure S1E). To further explore PKM2's role in NSPC differentiation, we induced NSPC differentiation post-transduction with shPKM2 or shNC lentivirus and assessed the proportions of $Tuj1^+$ (newborn neurons) and $GFAP^+$(astrocyte) cells. PKM2 knockdown NSPCs showed a lower proportion of $Tuj1^+$ cells compared to the control group, with no significant difference in $GFAP^+$ cell percentage between shPKM2 NSPCs and shNC NSPCs (Figure S1F). These findings suggest that PKM2 regulates NSPC proliferation and differentiation *in vitro*.

Next, to verify if this phenomenon occurs *in vivo*, we employed the same lentivirus to reduce PKM2 expression and assessed NSPC proliferation and differentiation using a standardized neurogenesis quantification methodology (Zhao and van Praag, 2020). Eight-week-old adult mice were stereotaxically injected with shPKM2 or shNC lentivirus into the hippocampal DG. Two weeks post-injection, abundant red fluorescence in the DG area confirmed successful lentivirus transduction (Figure 1E). In addition, we observed a significant decrease of relative PKM2 fluorescence intensity and reduced PKM2 intensity in RFP^+GFAP^+

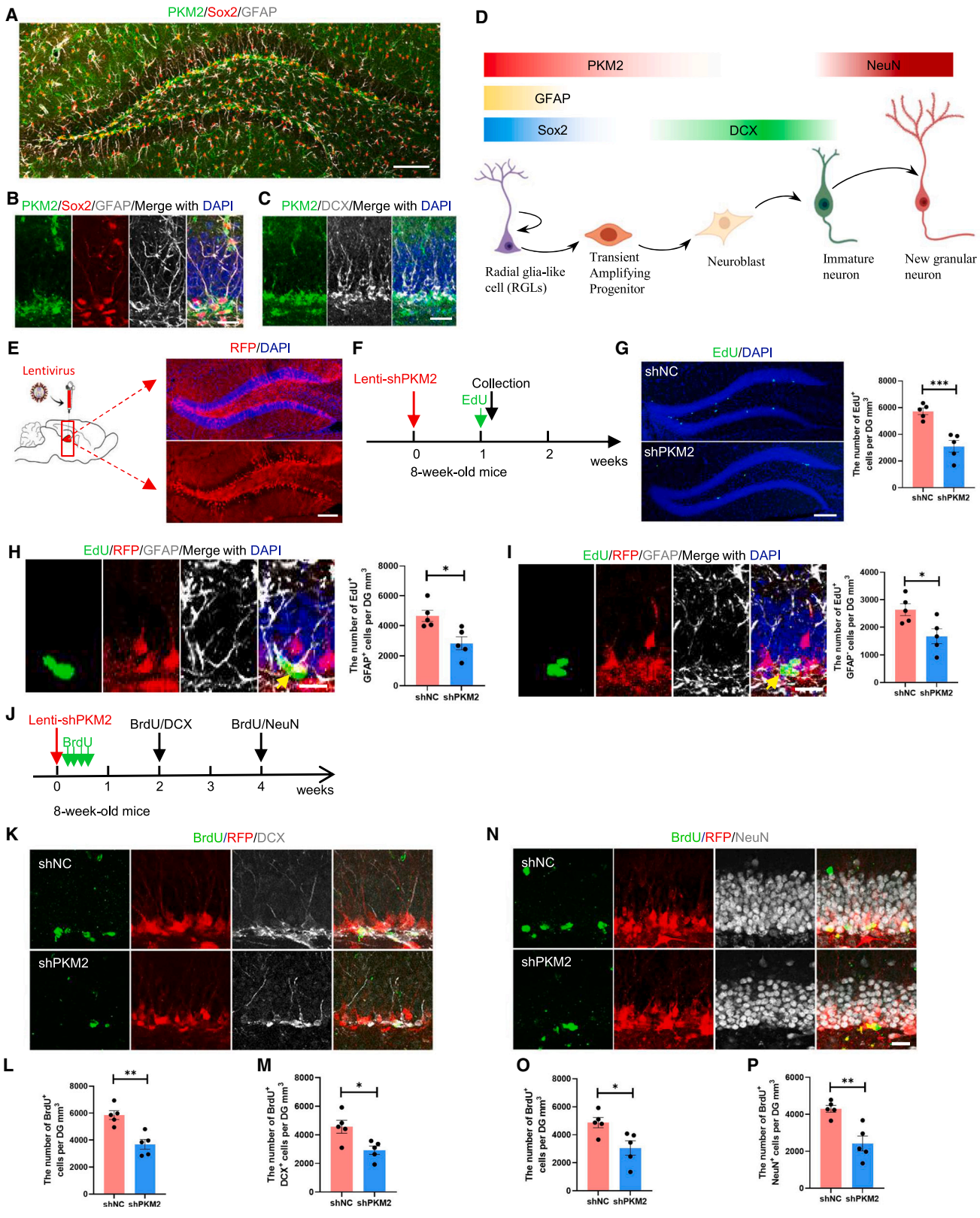

(legend on next page)

cells (with typical NSPC morphology) in the DG area of the shPKM2 group, suggesting high knockdown efficiency of lentivirus *in vivo* (Figure S1G). Compared to control mice, PKM2 knockdown mice exhibited a reduced number of EdU^+ cells per DG (Figures 1F and 1G). Moreover, PKM2 knockdown in the DG area resulted in decreased numbers of RGL NSPCs (EdU^+GFAP^+, typical NSPC morphology) (Figure 1H) and transiently amplifying progenitor cells (EdU^+GFAP^-) (Figure 1I), indicating that PKM2 deficiency negatively affects NSPC proliferation.

To assess PKM2's long-term effects on adult neurogenesis, mice received bromodeoxyuridine (BrdU) injections (Figure 1J). Compared to controls, the PKM2 knockdown group showed reduced numbers of newly differentiated immature neurons ($BrdU^+DCX^+$) (Figures 1K–1M) and mature neurons ($BrdU^+NeuN^+$) (Figures 1N–1P) per DG, suggesting compromised NSPC differentiation. These results collectively confirm that PKM2 deficiency leads to decreased proliferation of NSPCs and, consequently, to reduced differentiation of NSPCs in the adult hippocampus.

Deletion of PKM2 from NSPCs inhibits AHN

To specifically delete PKM2 in NSPCs and circumvent the extensive infection caused by lentivirus, we utilized a tamoxifen (TAM)-inducible $CreER^{T2}$ system. $PKM2^{fl/fl}$ mice were crossed with Nestin-$CreER^{T2}$ mice, generating $PKM2^{fl/fl}$; Nestin-$CreER^{T2}$ mice. In these mice, PKM2 could be conditionally knocked out in NSPCs upon TAM administration, creating PKM2 conditional knockout (cKO) mice. $PKM2^{fl/fl}$ littermates without Nestin-$CreER^{T2}$ served as controls (Figure 2A).

For *in vitro* experiments, primary mouse NSPCs were isolated and cultured from the DG of young adult $PKM2^{fl/fl}$; Nestin-$CreER^{T2}$ and control mice and then treated with 1 μM 4-hydroxytamoxifen (4-OH-TAM) to induce PKM2 ablation in NSPCs (Figure 2B). Immunofluorescence analysis revealed a significant decrease in EdU^+ NSPCs (proliferating cells) in the cKO group, consistent with our lentivirus findings (Figure 2C). Upon differentiation induction after 4-OH-TAM administration, the cKO NSPCs showed a lower proportion of $Tuj1^+$ cells compared to controls, with no significant difference in $GFAP^+$ cells (Figure 2D). These results underscore the critical role of PKM2 in NSPC proliferation and differentiation *in vitro*.

To investigate PKM2 deletion effects on neurogenesis *in vivo*, eight-week-old $PKM2^{fl/fl}$; Nestin-$CreER^{T2}$ and control mice received intraperitoneal TAM injections to conditionally knock out PKM2 in hippocampal NSPCs (Figure 2E). One week after the last day of TAM administration, western blot analysis confirmed a significant decrease in PKM2 expression in the hippocampus of cKO mice (Figure 2F).

Subsequently, we administered EdU intraperitoneally 2 h before sacrificing the mice to label proliferating cells. Compared to controls, cKO mice displayed reduced numbers of EdU^+ cells (Figure 2G), RGL NSPCs ($EdU^+GFAP^+Sox2^+$), and transiently amplifying progenitor cells ($EdU^+GFAP^-Sox2^+$) per DG (Figures 2H–2J), indicating that PKM2 deletion inhibits NSPC proliferation.

To assess PKM2's long-term effects on adult neurogenesis, mice received BrdU injections after TAM administration. The cKO mice exhibited lower numbers of newly differentiated immature neurons ($BrdU^+DCX^+$) (Figures 2K–2M) and mature neurons ($BrdU^+NeuN^+$) (Figures 2N–2P) per DG

Figure 1. PKM2 deficiency leads to compromised adult hippocampal neurogenesis

(A and B) Representative images of PKM2 expression in NSPCs ($Sox2^+$ $GFAP^+$) in the DG of 2-month-old wild-type mice. Scale bar for (A), 100 μm. Scale bar for (B), 20 μm.

(C) Representative images of PKM2 expression in immature neurons (DCX^+) in the DG of 2-month-old wild-type (WT) mice. Scale bar, 20 μm.

(D) Schematic diagram of the neural stem cell lineage showing stage-specific protein expression.

(E) Schematic diagram of PKM2 knockdown by intra-hippocampus injection of lentivirus in 8-week-old WT mice. The lentivirus expresses red fluorescent protein (RFP) with control shRNA (shNC) or shRNA targeting PKM2 (shPKM2). Scale bar, 100 μm.

(F) Timeline for assessing NSPC proliferation in 8-week-old wild-type mice injected with lentivirus expressing shPKM2 or shNC into the DG.

(G) Representative images and quantification of total proliferating cells (EdU^+) in the DG of the indicated groups. $n = 5$ animals per group. Scale bar, 100 μm.

(H) Representative images and quantification of EdU^+GFAP^+ radial glial-like (RGL) cells in the DG of the indicated groups. $n = 5$ animals per group. Scale bar, 20 μm.

(I) Representative images and quantification of EdU^+GFAP^- progenitor cells in the DG of the indicated groups. $n = 5$ animals per group. Scale bar, 20 μm.

(J) Timeline for assessing NSPC differentiation in 8-week-old WT mice injected with lentivirus expressing shPKM2 or shNC into the DG.

(K–M) Representative images and quantification of $BrdU^+$ cells and $BrdU^+DCX^+$ immature neurons in the DG of the indicated groups. $n = 5$ animals per group. Scale bar, 25 μm.

(N–P) Representative images and quantification of $BrdU^+$ cells and $BrdU^+NeuN^+$ mature newborn neurons in the DG of the indicated groups. $n = 5$ animals per group. Scale bar, 25 μm. All data in the bar graphs are presented as mean ± SEM. All statistical evaluation was performed using two-tailed unpaired Student's t test. Nonsignificant comparisons are not shown. $^*p < 0.05$, $^{**}p < 0.01$, $^{***}p < 0.001$, $^{****}p < 0.0001$.

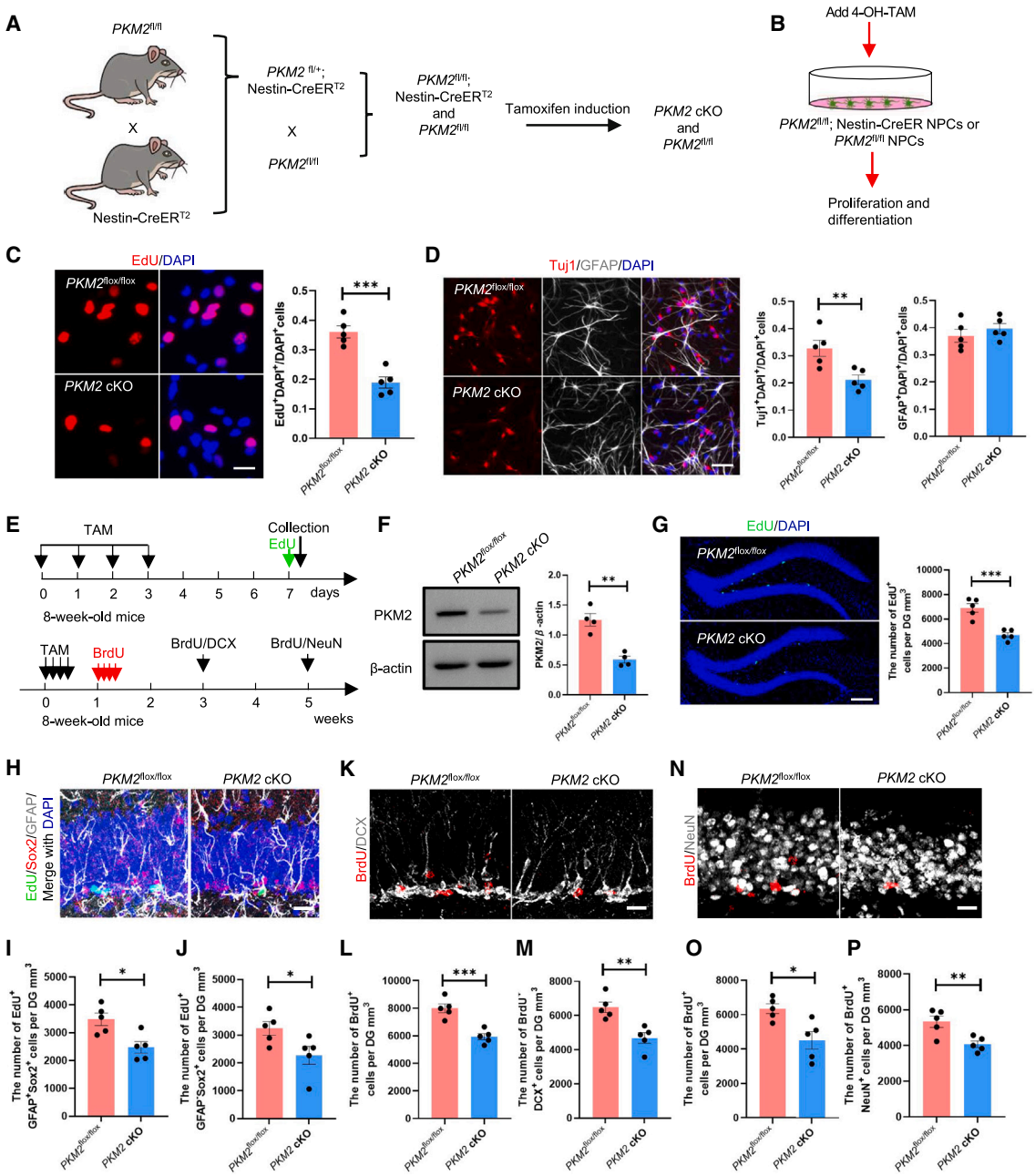

Figure 2. Deletion of PKM2 from NSPCs inhibits adult hippocampal neurogenesis

(A) Schematic diagram for generating conditional PKM2 knockout in NSPCs.

(B) Schematic diagram for analyzing NSPC proliferation and neuronal differentiation in *PKM2*$^{fl/fl}$ or cKO NSPCs.

(C) Representative images and quantification of NSPC proliferation (EdU) in *PKM2*$^{fl/fl}$ or cKO NSPCs. Scale bars, 20 μm. $n = 5$ experiments per group.

(D) Representative images and quantification of NSPC differentiation by neuronal (Tuj1) and glial (GFAP) markers in *PKM2*$^{fl/fl}$ or cKO NSPCs. Scale bars, 50 μm. $n = 5$ experiments per group.

(E) Experimental timeline for assessing the proliferation and differentiation of NSPCs in the DG of 8-week-old *PKM2*$^{fl/fl}$ or *PKM2*$^{fl/fl}$; Nestin-CreER^{T2} mice after TAM injection.

(F) PKM2 expression by immunoblotting of acutely dissected, unfixed hippocampal lysates from *PKM2* cKO and *PKM2*$^{fl/fl}$ mice. $n = 4$ independent experiments.

(legend continued on next page)

compared to control mice, suggesting impaired NSPC differentiation. To explore PKM2's effects on differentiated immature neurons (DCX^+), we administered BrdU before TAM injection (Figure S2B) and carried out immunofluorescent analysis. Interestingly, there was no difference in the numbers of $BrdU^+DCX^+$ (Figure S2C) and $BrdU^+NeuN^+$ (Figure S2D) cells between the two groups. Thus, we inferred that PKM2 deletion possibly did not affect the process from immature neurons ($BrdU^+DCX^+$) to mature neurons ($BrdU^+NeuN^+$).

Of note, a previous study suggested that reduced PKM2 levels lead to compensatory PKM1 expression and a metabolic shift from glycolysis to oxidative phosphorylation (Pan et al., 2022). To explore the influences of potential PKM1 ectopic expression during PKM2 knockout, we tested PKM1 expression in the hippocampus of $PKM2^{fl/fl}$ and cKO mice. Surprisingly, there was no difference in PKM1 expression in the two groups of mice (Figure S2A). Thus, the effects of PKM2 knockout on neurogenesis in our study are probably not related to the altered PKM1 expression. Collectively, these results demonstrate that PKM2 ablation significantly inhibits the proliferation and, consequently, contributes to decreased differentiation of NSPCs in the adult hippocampus.

Deletion of PKM2 in the hippocampus results in cognitive deficits in adult mice

Given the previous findings that PKM2 deficiency inhibits AHN, we hypothesized that a lack of PKM2 could result in defective cognitive functions. To test this, we conducted a series of behavioral assays to assess whether cognitive functions such as spatial learning and memory abilities were affected by PKM2 knockout. As previously described, 8-week-old adult $PKM2^{fl/fl}$; Nestin-$CreER^{T2}$ mice and control mice received TAM injections, and, 4 weeks after injection, they underwent behavioral testing in the order as labeled in our experimental timeline (Figure 3A).

In the open field test (OFT), there was no significant difference in total distance traveled or number of central zone crossings between the two groups, indicating that PKM2 deletion did not affect locomotor ability or anxiety-like behavior (Figures 3B–3D). However, in the novel object location (NOL) test (Figures 3E and 3F), the cKO group showed reduced preference for the object moved to a new location. Similarly, in the novel object recognition (NOR) test, the cKO group exhibited less exploration time for the new object compared to the control group (Figures 3G and 3H). These results collectively indicated impaired spatial learning and memory functions due to PKM2 knockout.

We also conducted an MWM test, training the mice to find a hidden platform submerged in opaque water. The cKO mice exhibited longer escape latencies to find the platform during the training period and fewer platform crossings in the probe test, where the platform was removed, suggesting impaired spatial memory (Figures 3I–3K). Furthermore, an RMWM task was performed 48 h after the initial probe test, requiring mice to find a hidden platform relocated to the opposite quadrant. The cKO mice took more time to find the hidden platform and had fewer platform crossings in the probe test compared to controls, revealing an impaired ability to extinguish the initial platform location memory and form new memory (Vorhees and Williams, 2006) (Figures 3L–3N).

Altogether, these findings indicate that the lack of PKM2 in the adult hippocampus results in impaired cognitive functions, including spatial learning and memory abilities.

L-lactate supplementation can rescue PKM2-deficiency-induced inhibition of neurogenesis

PKM2 plays a critical role in glycolysis by catalyzing the transfer of PEP to pyruvate, producing ATP (Bond et al., 2015). Since pyruvate is the upstream substrate for L-lactate production, PKM2 deficiency could logically lead to decreased L-lactate levels (Figure 4A). Given that L-lactate has been shown to promote AHN (Lev-Vachnish et al., 2019), we hypothesized that L-lactate supplementation might partially rescue the negative effects of PKM2 deficiency on AHN.

To demonstrate that PKM2 deficiency leads to reduced L-lactate levels, we measured the L-lactate concentration in the supernatant of cultured NSPCs. Primary mouse NSPCs were cultured and infected with shPKM2 or shNC lentivirus, with culture medium replaced 24 h before

(G) Representative images and quantification of total proliferating cells (EdU^+) in the DG of the indicated groups. $n = 5$ animals per group. Scale bars, 100 μm.

(H–J) Representative images and quantification of $EdU^+GFAP^+Sox2^+$ radial glial-like (RGL) cells and $EdU^+GFAP^-Sox2^+$ transiently amplifying progenitor cells in the DG of the indicated groups. $n = 5$ animals per group. Scale bars, 25 μm.

(K–M) Representative images and quantification of $BrdU^+$ cells and $BrdU^+DCX^+$ immature neurons in the DG of the indicated groups. $n = 5$ animals per group. Scale bars, 25 μm.

(N–P) Representative images and quantification of $BrdU^+$ cells and $BrdU^+NeuN^+$ mature newborn neurons in the DG of the indicated groups. $n = 5$ animals per group. Scale bars, 25 μm. All data in the bar graphs are presented as mean ± SEM. All statistical evaluation was performed using two-tailed unpaired Student's t test. Nonsignificant comparisons are not shown. $^*p < 0.05$, $^{**}p < 0.01$, $^{***}p < 0.001$, $^{****}p < 0.0001$.

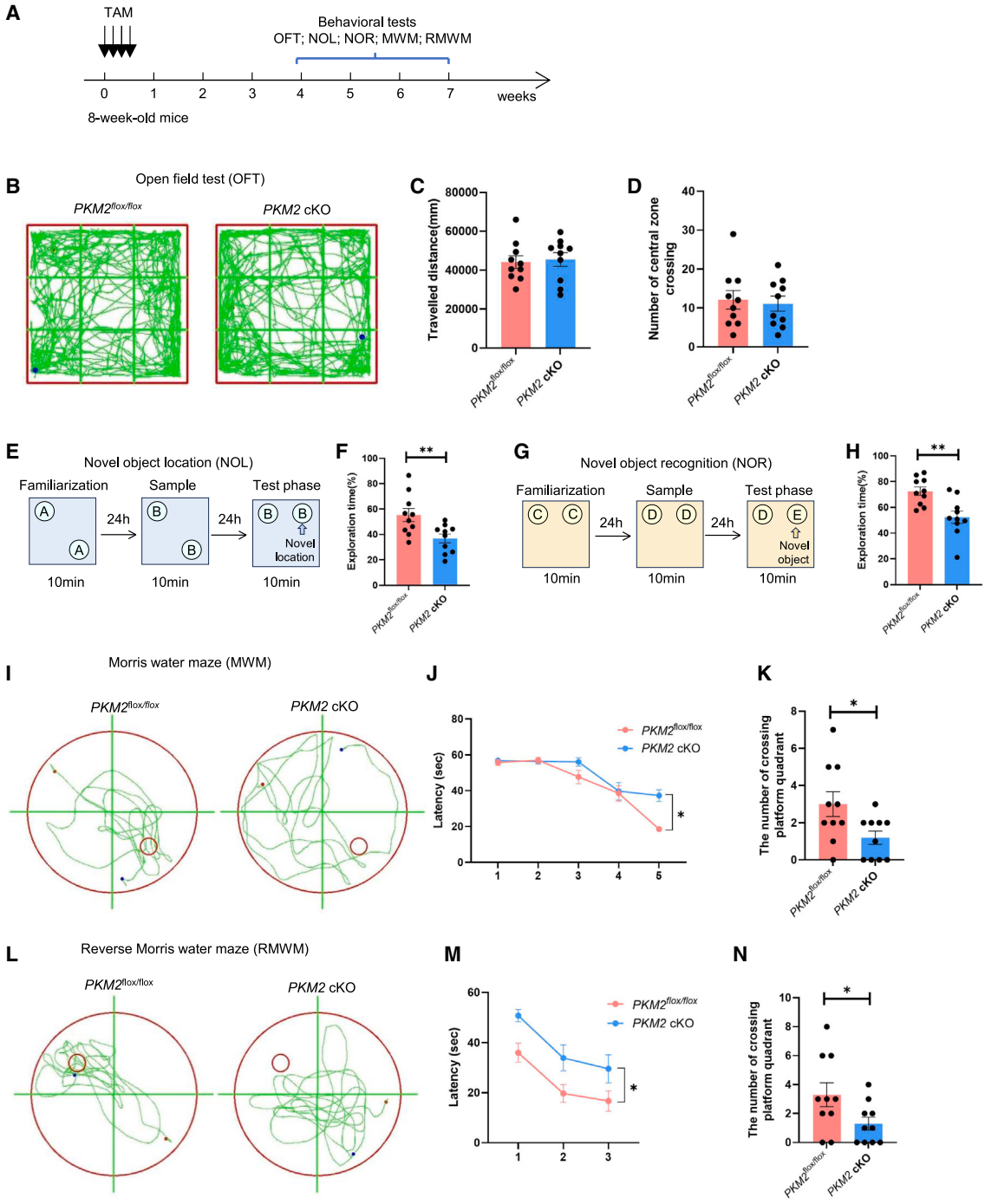

Figure 3. Deletion of PKM2 in the hippocampus results in cognitive deficits in adult mice

(A) Timeline of experiments to assess behavioral performance in 8-week-old mice with conditional knockout of PKM2 by intraperitoneal tamoxifen injection. The OFT (1 day), NOL (3 days), NOR (3 days), MWM (6 days), and RMWM (4 days) behavioral tests were conducted sequentially at weeks 4–6.

(B) Representative movement paths in the open field test for the indicated groups.

(C and D) Quantification of total distance traveled and number of center area crossings in the open field test. n = 10 animals per group.

(E) Schematic diagram of the novel object location (NOL) test.

(F) Quantification of exploration time for the novel object in the NOL. n = 10 animals per group.

(G) Schematic diagram of the novel object recognition (NOR) test.

(legend continued on next page)

supernatant collection. The shPKM2 group showed lower L-lactate levels compared to controls, confirming our hypothesis that reduced PKM2 expression decreases L-lactate levels (Figures S2E and S2F). As lactate dehydrogenase A (LDHA) catalyzes the conversion from pyruvate to lactate, and its expression can be regulated by the PKM2 dimer (Palsson-McDermott et al., 2015), we wondered whether the decreased lactate levels were due to a decline in LDHA expression. We performed western blot analysis and observed no difference in NSPCs' LDHA levels between shNC and shPKM2 groups (Figure S2G). Thus, the reduction in lactate levels after PKM2 knockdown can be mainly resulted from a deficiency in substrate, rather than an alteration in LDHA expression level.

We then treated shNC and shPKM2 NSPCs with 20 mM L-lactate or phosphate-buffered saline (PBS) as a negative control. As expected, PKM2 knockdown led to fewer EdU$^+$ NSPCs (proliferating cells) (Figure S2H) and a lower proportion of Tuj1$^+$ cells (newborn neurons) compared to the shNC group (Figure S2I). L-lactate administration restored the proliferation and differentiation of shPKM2 NSPCs to near-normal levels and improved these parameters in shNC NSPCs. However, there was no difference in the percentage of GFAP$^+$ (astrocyte) cells among the four groups (Figures S2H and S2I).

For *in vivo* tests, following stereotaxical lentivirus injections, BrdU or EdU labeling was performed at the indicated time points to quantify NSPC proliferation and neuronal differentiation. L-lactate was administered intraperitoneally at 1 g/kg to mimic physiological L-lactate levels post-exercise (So et al., 2017). L-lactate treatment increased the numbers of EdU$^+$ cells, RGL NSPCs (EdU$^+$GFAP$^+$Sox2$^+$), and transiently amplifying progenitor cells (EdU$^+$GFAP$^-$Sox2$^+$) per DG (Figures S3D–S3G). It also enhanced the numbers of newly differentiated immature neurons (BrdU$^+$DCX$^+$) (Figures S3H–S3J) and mature neurons (BrdU$^+$NeuN$^+$) (Figures S3K–S3M) per DG in both shNC and shPKM2 groups.

To further validate these findings, we repeated the experiments with PKM2 cKO cultured NSPCs and mice. As before, lactate levels were lower in cKO NSPCs compared to controls (Figures 4B and 4C). L-lactate treatment increased the number of EdU$^+$ (proliferating) cells (Figure 4D) and the proportion of Tuj1$^+$ cells (differentiated neurons) in both cKO and control groups *in vitro* (Figure 4E). *In vivo*, following TAM injection, BrdU or EdU labeling, and L-lactate administration at 1 g/kg (Figures 4F and 4G), L-lactate-treated *PKM2*$^{fl/fl}$ mice showed increased numbers of EdU$^+$ cells, RGL NSPCs (EdU$^+$GFAP$^+$Sox2$^+$), and transiently amplifying progenitor cells (EdU$^+$GFAP$^-$Sox2$^+$) per DG compared to vehicle-treated mice (Figures 4H–4K). This effect was also observed in PKM2 cKO mice. Additionally, L-lactate treatment elevated the number of newly differentiated immature neurons (BrdU$^+$DCX$^+$) (Figures 4L–4N) and mature neurons (BrdU$^+$NeuN$^+$) (Figures 4O–4Q) per DG in both control and PKM2 cKO mice. In conclusion, these results validate that L-lactate supplementation can promote AHN and mitigate the detrimental effects of PKM2 depletion.

L-lactate can rescue cognitive functions in the condition of PKM2 deletion

Based on our findings that L-lactate facilitates AHN and ameliorates the neurogenesis defects caused by PKM2 deletion, it is plausible that L-lactate supplementation could improve cognitive functions. Eight-week-old *PKM2*$^{fl/fl}$; Nestin-CreER^{T2} mice and control mice received TAM injections, followed by L-lactate administration prior to behavioral testing (Figure 5A).

In the OFT, there was no significant difference in total distance traveled or the number of central zone crossings between the four groups, indicating that locomotor ability and anxiety-like behavior were not affected by the treatments (Figures S3A–S3C). Consistent with our previous results, in both the NOL test and the NOR test, cKO mice showed reduced preference for the new object compared to control mice. The recognition index, reflected by the exploration time of the new object, improved with L-lactate administration. Although L-lactate tended to enhance performance in control mice during the NOL and NOR tests, the improvement was not statistically significant (Figures 5B and 5C).

Furthermore, in the MWM test and the RMWM task, cKO mice exhibited longer escape latencies and fewer platform crossings, as well as lesser time spent in the platform quadrant. L-lactate administration partially alleviated these behavioral deficits. However, L-lactate did not significantly improve performance in control mice in the MWM or RMWM tests, although there was a trend toward shorter

(H) Quantification of exploration time for the novel object in the NOR. $n = 10$ animals per group.
(I) Representative Morris water maze (MWM) movement paths in the probe test for the indicated groups.
(J and K) Quantification of MWM escape latencies to find the platform and platform quadrant crossing numbers. $n = 10$ animals per group.
(L) Representative reverse Morris water maze (RMWM) movement paths in the probe test for the indicated groups.
(M and N) Quantification of RMWM escape latencies to find the platform and platform quadrant crossing numbers. $n = 10$ animals per group.
All data in the bar graphs are presented as mean ± SEM. For (C), (D), (F), (H), (K), and (N), statistical evaluation was performed using two-tailed unpaired Student's t test. For (J) and (M), significance was evaluated with two-way ANOVA and Tukey's multiple comparisons test. Nonsignificant comparisons are not shown. $^*p < 0.05$, $^{**}p < 0.01$, $^{***}p < 0.001$, $^{****}p < 0.0001$.

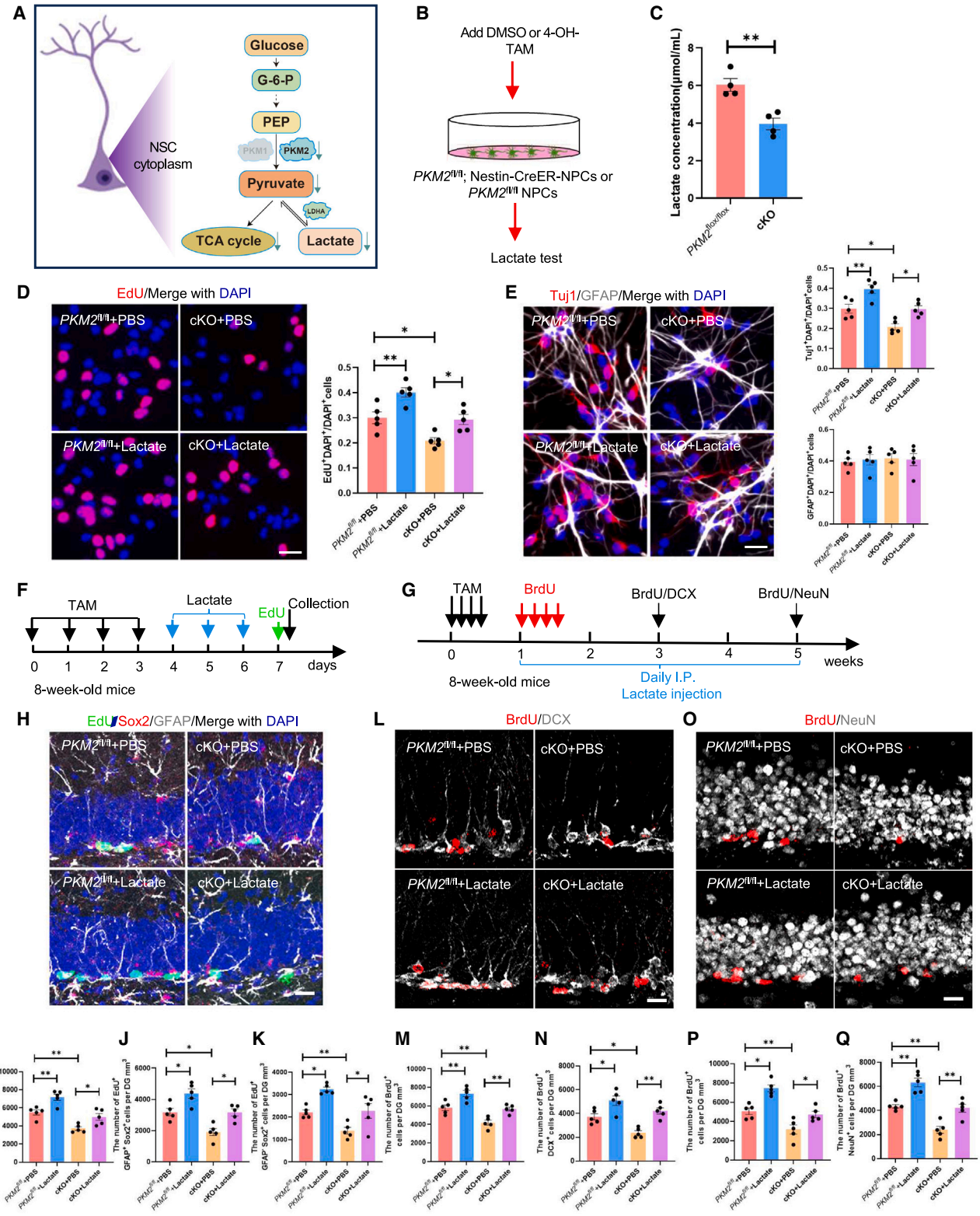

Figure 4. L-lactate supplementation can rescue PKM2-deficiency-induced inhibition of neurogenesis

(A) Schematic diagram of lactate production from glucose.

(B) Schematic diagram for analyzing lactate concentration in the supernatant of *PKM2*$^{fl/fl}$ or cKO NSPCs.

(legend continued on next page)

escape latencies, more platform crossings, and more time spent in the platform quadrant (Figures 5D–5K).

In summary, these results demonstrate that L-lactate can mitigate the negative effects on cognitive functions caused by PKM2 deletion, highlighting its potential therapeutic role in enhancing cognitive performance in conditions of impaired neurogenesis.

L-lactate exerts its effect of restoring AHN in PKM2-deficient condition via MCT2

Previous research indicates that extracellular L-lactate is transported into neurons via MCT2 and converted to pyruvate by LDHA, serving as a substrate for oxidative phosphorylation. Besides its role in energy metabolism, L-lactate activates downstream signaling pathways, regulating growth factor production and gene expression related to neural plasticity. HCAR1 (G-protein-coupled receptor, GPR81) is an L-lactate receptor expressed in the brain, which plays a crucial role in mediating L-lactate's effects.

Studies have demonstrated abundant expression of both HCAR1 and MCT2 on NSPCs (Lambertus et al., 2021; Lev-Vachnish et al., 2019). Thus, to investigate the mechanisms by which L-lactate influences AHN, we designed lentiviruses expressing shRNA targeting MCT2 or HCAR1, along with green fluorescent protein (GFP), to knockdown these proteins (Figure 6A). Western blot analysis confirmed significant reductions in MCT2 and HCAR1 expression in cultured NSPCs *in vitro*, indicating effective knockdown efficiency (Figures S4A and S4B).

Initially, wild-type (WT) cultured NSPCs were infected with these lentiviruses to observe their effects on proliferation and differentiation. Immunofluorescence results showed that shMCT2 or shHCAR1 lentivirus did not influence proliferation or differentiation ratios compared to the control group, suggesting that MCT2 and HCAR1 do not directly affect neurogenesis in the absence of L-lactate (Figures S4C and S4D). Upon L-lactate administration to the three groups of NSPCs, we observed an increase in EdU^+ NSPCs (proliferating cells) and $Tuj1^+$ cells (newborn neurons) in the shNC group. However, L-lactate supplementation did not enhance proliferation or differentiation in the MCT2 knockdown group. Surprisingly, the shHCAR1 group showed similar results to the shNC group after L-lactate treatment, indicating that HCAR1 is not essential for L-lactate's beneficial effects on NSPC proliferation or differentiation (Figures S4E–S4I).

For *in vivo* tests, WT adult mice received intraperitoneal L-lactate injections after lentivirus injections, with EdU and BrdU labeling (Figures 6C and 6H). Green fluorescence in the DG area two weeks post-injection confirmed successful lentivirus transduction (Figure 6B). Compared to vehicle-treated shNC mice, the L-lactate-treated shNC group showed increased numbers of EdU^+ cells, RGL NSPCs ($EdU^+GFAP^+Sox2^+$), and transiently amplifying progenitor cells ($EdU^+GFAP^-Sox2^+$) per DG (Figures 6D–6G). Similar results were found in the shHCAR1 group. Additionally, L-lactate increased the number of newly differentiated immature neurons ($BrdU^+$ DCX^+) (Figures 6I–6K) and mature neurons ($BrdU^+$ $NeuN^+$) (Figures 6L–6N) per DG in both shNC and shHCAR1 groups. However, MCT2 knockdown negated L-lactate's beneficial effects on NSPC proliferation and differentiation. These findings verified that MCT2 is indispensable for L-lactate's promotion of AHN.

To further confirm our findings, we conducted similar experiments on PKM2 cKO cultured NSPCs and mice. Consistent with WT results, shHCAR1 or shMCT2 lentivirus infection alone did not affect neurogenesis activity (Figures S5A and S5B). L-lactate administration elevated proliferation and differentiation ratios in shNC and shHCAR1 groups but had no effect on NSPCs with MCT2 knockdown,

(C) Quantification of lactate concentration in the supernatant of the indicated groups. $n = 4$ per group.
(D) Representative images and quantification of NSPC proliferation (EdU) in the indicated groups. Scale bars, 25 μm; $n = 5$ experiments per group.
(E) Representative images and quantification of NSPC differentiation by neuronal (Tuj1) and glial (GFAP) markers in the indicated groups. Scale bars, 25 μm; $n = 5$ experiments per group.
(F) Experimental timeline for assessing NSPC proliferation in the DG of 8-week-old $PKM2^{fl/fl}$ or $PKM2^{fl/fl}$; Nestin-CreERT2 mice after tamoxifen (TAM) injection.
(G) Experimental timeline for assessing NSPC differentiation in the DG of 8-week-old $PKM2^{fl/fl}$ or $PKM2^{fl/fl}$; Nestin-$CreER^{T2}$ mice after tamoxifen (TAM) injection.
(H–K) Representative images and quantification of total proliferating cells (EdU^+), $EdU^+GFAP^+Sox2^+$ radial glial-like (RGL) cells, and $EdU^+GFAP^-Sox2^+$ transiently amplifying progenitor cells in the DG of the indicated groups. $n = 5$ animals per group. Scale bars, 25 μm.
(L–N) Representative images and quantification of $BrdU^+$ cells and $BrdU^+DCX^+$ immature neurons in the DG of the indicated groups. $n = 5$ animals per group. Scale bars, 25 μm.
(O–Q) Representative images and quantification of $BrdU^+$ cells and $BrdU^+NeuN^+$ mature newborn neurons in the DG of the indicated groups. $n = 5$ animals per group. Scale bars, 25 μm. All data in the bar graphs of are presented as mean ± SEM. For (C), statistical evaluation was performed using two-tailed unpaired Student's t test. For (D), (E), (I), (J), (K), (M), (N), (P), and (Q), statistical evaluation was performed using one-way ANOVA and Tukey's *post hoc* multiple comparisons. Nonsignificant comparisons are not shown. $^*p < 0.05$, $^{**}p < 0.01$, $^{***}p < 0.001$, $^{****}p < 0.0001$.

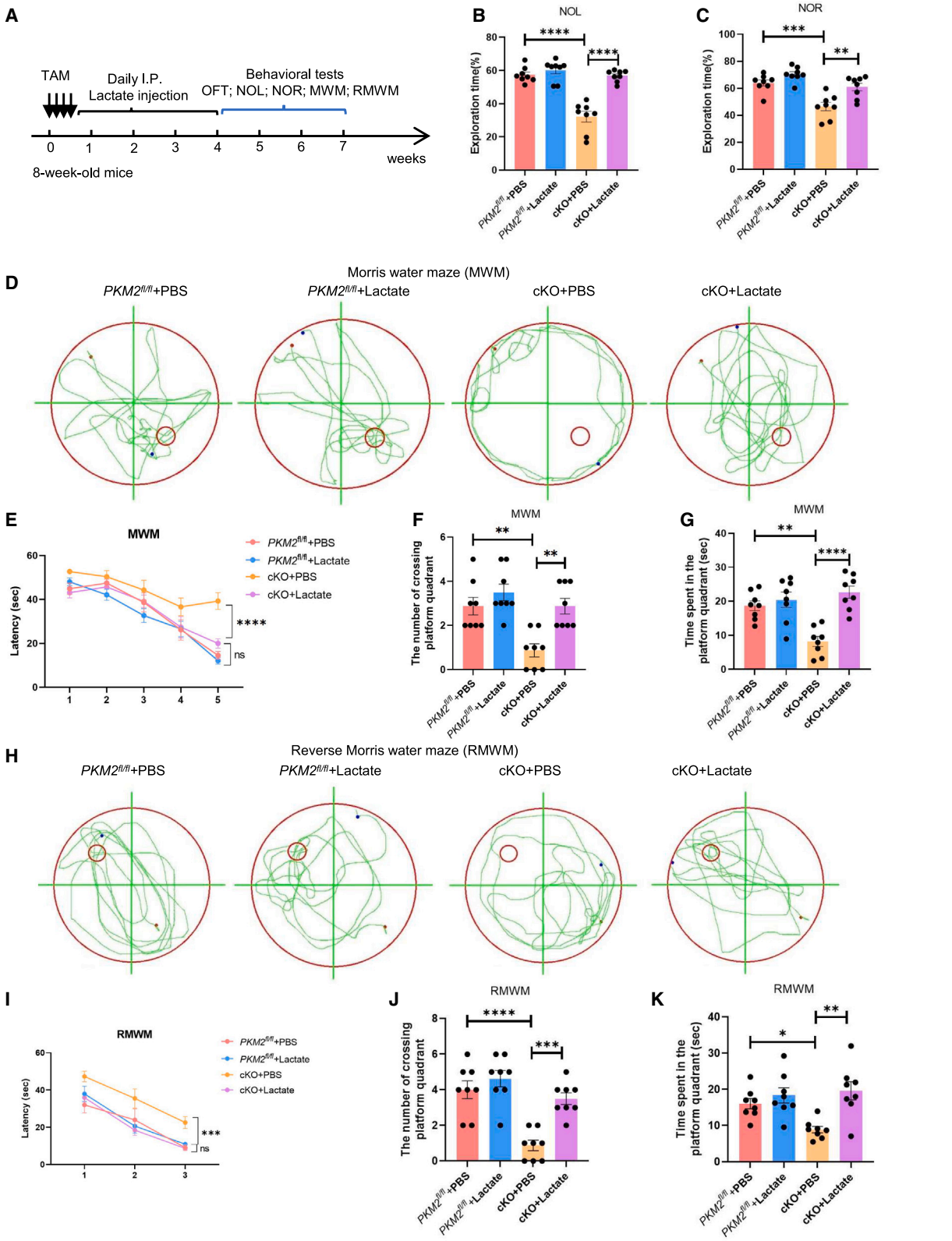

(legend on next page)

both *in vitro* and *in vivo* (Figures S5C–S5G and S6A–S6J). Ultimately, our findings confirmed that L-lactate's role in restoring AHN in PKM2-deficient conditions is markedly dependent on MCT2.

DISCUSSION

AHN, the formation of new functional neurons from NSPCs in the DG area of the hippocampus, is closely related to cognitive functions and can be influenced by numerous factors. Our study highlighted the critical role of PKM2 in AHN. We demonstrated that PKM2 ablation reduced NSPC proliferation and differentiation, while L-lactate supplementation could rescue neurogenesis. Additionally, we validated that L-lactate exerts its function of restoring neurogenesis through MCT2.

Research shows that the PKM gene encodes transcripts containing either exon 9 or exon 10, resulting in two isoforms: PKM1 mRNA and PKM2 mRNA, produced by mRNA splicing (Chen et al., 2012). PKM1 is expressed in most adult tissues with high energy demands, such as muscle and brain, while PKM2 is mainly found in proliferative cells like embryonic cells, stem cells, and tumor cells (Nayak et al., 2021). The PKM2 dimer is catalytically inactive, preventing pyruvate production and leading to the accumulation of upstream glycolytic intermediates, which are redirected to biosynthetic pathways to support cell proliferation (Liu et al., 2021). In contrast, the tetramer form of PKM2 is an active pyruvate kinase, and both forms exist in proliferating cells (Mazurek et al., 2005). The balance between tetramer and dimer forms is crucial for proliferating cells, balancing energy and substrate demands for biosynthesis.

Our immunofluorescence results showed high PKM2 expression in NSPCs, with PKM2 ablation negatively impacting AHN, likely due to disrupted energy metabolism and anabolic processes. Some studies suggest that reduced PKM2 levels lead to compensatory PKM1 expression and a metabolic shift from glycolysis to oxidative phosphorylation (Pan et al., 2022). However, in our study, we did not observe a significant increase in the PKM1 expression level after knocking out PKM2, and the reason underlying this phenomenon is unclear. Therefore, it is likely that the negative effects of PKM2 knockout on neurogenesis are mediated by other mechanisms rather than PKM1.

Previous studies have shown that PKM2 can improve cognitive functions in age-related diseases like Alzheimer's disease (AD). It is believed that aerobic glycolysis, an important process of glucose metabolism, is evidently declined in AD (Liu et al., 2017). Additionally, electroacupuncture treatment can activate AMP-activated protein kinase, a key regulator of energy metabolism, thereby facilitating the expression of glycolysis-related proteins in the hippocampus, including PKM2, to improve memory and other cognitive functions (Li et al., 2021). But it is still unclear whether PKM2's ability to improve cognitive functions in AD is related to neurogenesis.

PKM2 has also been demonstrated to be involved in multiple signaling pathways relating to proliferation, differentiation, or migration. A previous study found that, in neural progenitor cell cultures, PKM2 increased the expression level of key adhesion/migration factors such as integrin β1 and the phosphorylation (activation) of focal adhesion kinase, which accelerates migration (Chen et al., 2018). Furthermore, PKM2 ameliorates symptoms of post-ischemic stroke depression by activating VEGF to mediate the MAPK/ERK pathway, thus maintaining the survival of oligodendrocytes (Feng et al., 2022).

Aside from age and stress, the effects of physical exercise on cognitive functions and neurogenesis have long been studied, which appears to be primarily mediated by changes in brain-derived neurotrophic factor, VEGF, lactate, and several other proteins in the brain (Ben-Zeev et al., 2022). Thus, in our study, to elucidate downstream effects of PKM2 knockout, we focused on lactate, which is an

Figure 5. L-lactate can rescue cognitive functions in the condition of PKM2 deletion

(A) Timeline of experiments to assess behavioral performance in 8-week-old mice with conditional knockout of PKM2 by TAM injection, followed by lactate administration. The OFT, NOL, NOR, MWM, and RMWM behavioral tests were conducted sequentially at weeks 4–6.

(B) Quantification of exploration time for the novel object in the NOL. $n = 8$ animals per group.

(C) Quantification of exploration time for the novel object in the NOR. $n = 8$ animals per group.

(D) Representative Morris water maze (MWM) movement paths in the probe test for the indicated groups.

(E–G) Quantification of MWM escape latencies to find the platform, platform quadrant crossing numbers, and time spent in the platform quadrant. $n = 8$ animals per group.

(H) Representative reverse Morris water maze (RMWM) movement paths in the probe test for the indicated groups.

(I and J) Quantification of RMWM escape latencies to find the platform, platform quadrant crossing numbers, and time spent in the platform quadrant. $n = 8$ animals per group.

(K) All data in the bar graphs are presented as mean ± SEM. Statistical evaluation of (B), (C), (F), (G), (J), and (K) was performed using one-way ANOVA and Tukey's *post hoc* multiple comparisons; for (E) and (I), significance was evaluated with two-way ANOVA and Tukey's multiple comparisons test. Nonsignificant comparisons are not shown. $^{*}p < 0.05$, $^{**}p < 0.01$, $^{***}p < 0.001$, $^{****}p < 0.0001$.

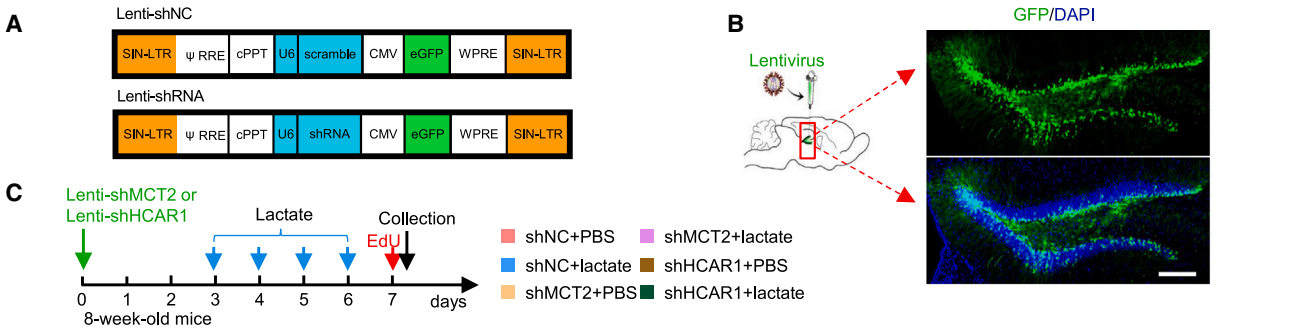

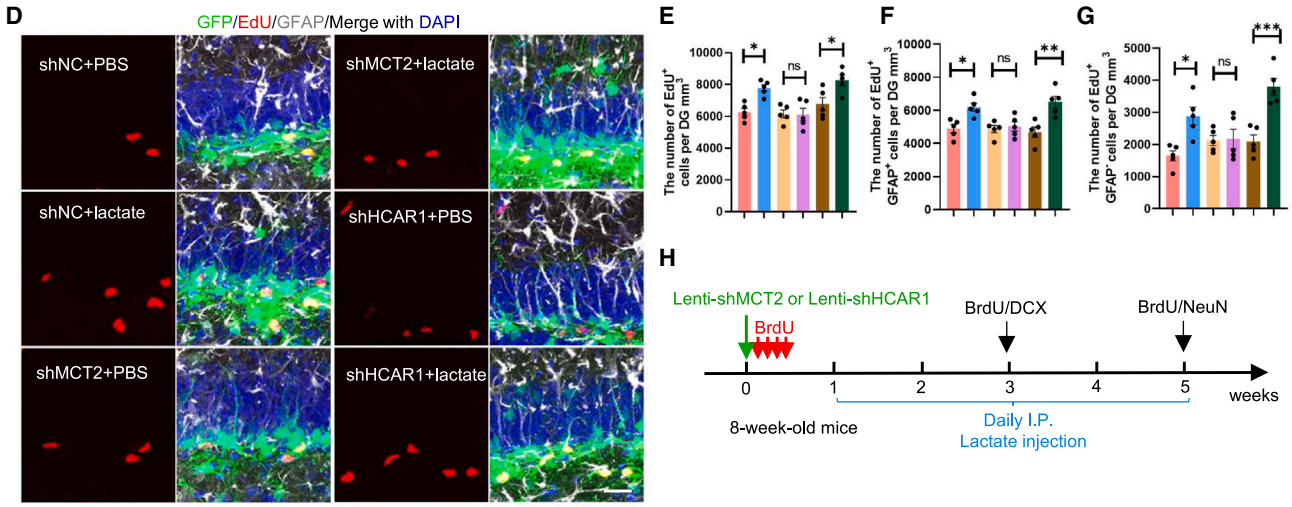

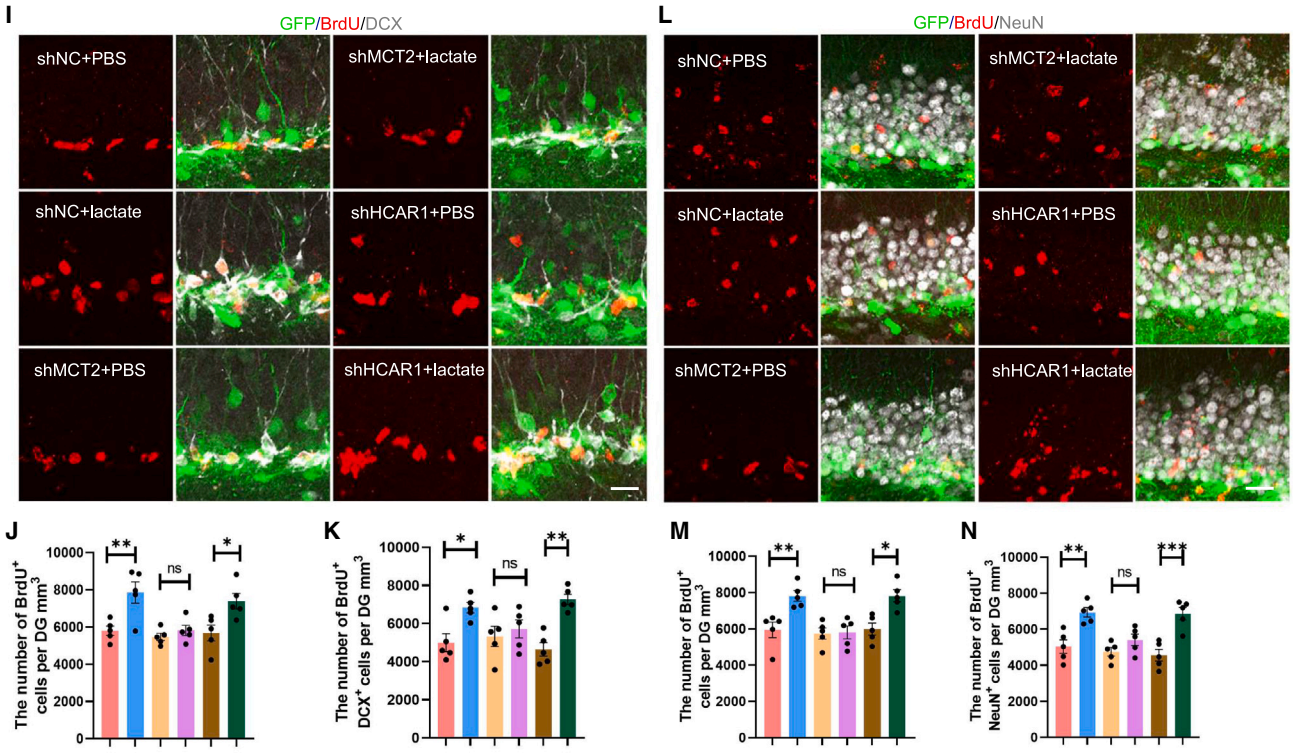

(legend on next page)

LDHA-mediated metabolite of pyruvate. The PKM2 dimer can translocate to the nucleus and regulate the expression of glycolysis-related genes, including LDHA, GLUT1, and PDK1, contributing to the Warburg effect in tumors (Palsson-McDermott et al., 2015). However, in our study, we did not observe a decrease in the expression level of LDHA after PKM2 deletion, possibly because LDHA is regulated by numerous factors except for PKM2 (Sharma et al., 2022). Therefore, we can exclude the influence of LDHA and attribute the reduced lactate production to a lack of substrate. Neurons use lactate produced by astrocytes during intense synaptic activity, transported via MCT2 and converted back to pyruvate by LDH1 for oxidative phosphorylation (Deitmer et al., 2019). Apart from acting as a substrate for energy metabolism, lactate also modulates pathways involved in neurogenesis, angiogenesis, neuronal excitability, and plasticity, essential for the survival of new neurons (Zhou et al., 2018).

Our study confirmed that lactate supplementation restored AHN and improved cognitive functions after PKM2 deletion. However, MCT2 knockdown abrogated these benefits, indicating a critical role of this lactate transporter in these processes. Lactate transported into NSPCs via MCT2 likely compensates for reduced pyruvate production due to PKM2 deficiency, meeting the energy demands. Lactate also increases glucose-6-phosphate dehydrogenase activity, key to the pentose phosphate pathway (PPP), promoting cell proliferation and differentiation (Xu et al., 2016). *De novo* lipogenesis, critical for NSPC proliferation, relies on nicotinamide adenine dinucleotide phosphate (NADPH) provided by the PPP, with lactate serving as a carbon source (Jin et al., 2018). Interestingly, control mice with lactate supplementation showed slightly improved hippocampal neurogenesis and cognitive performance, but the improvement was not statistically significant. This could be due to the high baseline performance of healthy young adult mice in cognitive tests, such as the MWM.

Research showed that MCT2 inhibition abolishes L-lactate's effects on neurogenesis (Lev-Vachnish et al., 2019). However, MCT2 knockdown alone did not affect NSPC proliferation or differentiation, suggesting extrinsic lactate transportation is not crucial under normal conditions. In our study, HCAR1 knockdown did not influence AHN in the DG area, either with or without lactate supplementation. This is supported by former studies indicating that HCAR1-dependent neurogenesis is specific to the SVZ but not to the DG of hippocampus (Kennedy et al., 2022).

In summary, our study demonstrated the indispensable role of PKM2 in AHN and that lactate supplementation is able to restore neurogenesis in PKM2-deficiency conditions via MCT2. Mounting evidence indicates that, with prolonged physical exercise, oxygen level decreases and promotes the conversion from pyruvate to lactate to produce sufficient energy. Then lactate is released into circulation and leads to an influx of lactate into the brain (Quistorff et al., 2008). As we discussed before, lactate is now identified as an important substrate for energy metabolism and a signaling molecule. Thus, our research on PKM2 and lactate provides some insights into the mechanisms by which voluntary physical exercise enhances AHN (van Praag et al., 2005).

EXPERIMENTAL PROCEDURES

Animals

All animal husbandry and experiments were performed in accordance with the National Institutes of Health Guide for the Care and Use of Laboratory Animals and were approved by the Institutional Animal Care and Use Committee of Sun Yat-sen University. Mice were kept under pathogen-free conditions at a constant temperature of 22°C–26°C and maintained on a 12-h light/12-h dark cycle. They were provided with food and water *ad libitum*. In behavioral assays, we used 8-week-old male mice, while, in other non-behavioral experiments, both male and female mice were used. All C57BL/6 mice were purchased from GemPharmatech.

Figure 6. L-lactate restores adult hippocampal neurogenesis in PKM2-deficient conditions via MCT2

(A) Lentiviral vectors expressing shRNAs for MCT2 (shMCT2), HCAR1 (shHCAR1), or a control shRNA (shNC), with eGFP coexpression.

(B) Schematic diagram of MCT2 or HCAR1 knockdown by intra-hippocampal injection of lentivirus in 8-week-old wild-type mice. The lentivirus expresses eGFP with control shRNA (shNC), shRNA targeting MCT2 (shMCT2), or HCAR1 (shHCAR1). Scale bars, 100 μm.

(C) Experimental timeline for assessing NSPC proliferation in the DG of 8-week-old WT mice after lentivirus injection.

(D–G) Representative images and quantification of total proliferating cells (EdU^+), $EdU^+GFAP^+Sox2^+$ radial glial-like (RGL) cells, and $EdU^+GFAP^-Sox2^+$ transiently amplifying progenitor cells in the DG of the indicated groups. $n = 5$ animals per group.

(H) Experimental timeline for assessing NSPC differentiation in the DG of 8-week-old WT mice after lentivirus injection.

(I–K) Representative images and quantification of $BrdU^+$ cells and $BrdU^+DCX^+$ immature neurons in the DG of the indicated groups. $n = 5$ animals per group.

(L–N) Representative images and quantification of $BrdU^+$ cells and $BrdU^+NeuN^+$ mature newborn neurons in the DG of the indicated groups. $n = 5$ animals per group. All data in the bar graphs are presented as mean ± SEM. Statistical evaluation was performed using one-way ANOVA and Tukey's *post hoc* multiple comparisons. Nonsignificant comparisons are not shown. $^*p < 0.05$, $^{**}p < 0.01$, $^{***}p < 0.001$, $^{****}p < 0.0001$.

Primary mouse NSPC isolation and culturing

The mouse NSPCs were isolated from the DG of 8-week-old WT C57BL/6 mice largely based on a published protocol (Guo et al., 2012). Briefly, after microdissection and enzymatic digestion of the DG, trypsin inhibitor (soybean) (YuanYe Biology, S10088) was added to terminate digestion. Then, we centrifuged the digested tissue chunks at 1,000*g* for 5 min and discarded the supernatant. We next resuspended it with proliferation medium consisting of Neurobasal medium (Gibco, 21103049) containing 2% B27 supplement (Gibco, 17504044), 20 ng/mL epidermal growth factor (PeproTech, A2306), 20 ng/mL basic fibroblast growth factor 2 (PeproTech, K1606), 2 mM L-glutamine (Gibco, 25030-081), and 1% penicillin-streptomycin (Gibco, 15140-122). The suspending neurospheres were incubated in a 5% CO_2 incubator (Thermo Fisher Scientific, 371) at 37°C, and half of the medium was replaced every 2 days.

EdU and BrdU administration for analysis of NSPC proliferation and differentiation

For the analysis of NSPC proliferation in the DG of the hippocampus, mice were intraperitoneally injected with EdU at a dose of 100 mg/kg 2 h before being sacrificed. Then we used the EdU Cell Proliferation Kit (Beyotime, C0078L) to detect EdU according to the manufacturer's protocol. For the analysis of NSPC differentiation, mice were intraperitoneally injected with BrdU at a dose of 100 mg/kg and were sacrificed after 2 or 4 weeks based on the experimental design.

Statistical analysis

The sample size in our experiments was not predetermined by any statistical methods, and the number of sample sizes is described in the figure legends. The normality of our data distribution was determined by a Shapiro-Wilk normality test, with $p < 0.05$ indicating a nonnormal distribution. For the data confirmed to be normally distributed, we used F test to examine the homogeneity of variance and unpaired two-tailed Student's t test for two-group comparisons. Bartlett's test to compare variances and one-way ANOVA were used for multiple-group comparisons, followed by Tukey's *post hoc* test. Additionally, two-way ANOVA was used for the analysis of MWM latency. For data that were not normally distributed, non-parametric alternatives such as Mann-Whitney or Kruskal-Wallis test were used. For data that did not pass the homogeneity test of variance, Student's t test with Welch's correction or Welch's ANOVA test was used. Our data were expressed as mean ± SEM, and significance was set as $^{*}p < 0.05$, $^{**}p < 0.01$, $^{***}p < 0.001$, and $^{****}p < 0.0001$. All statistical analyses were performed in GraphPad Prism 9 (GraphPad Software).

Additional procedures

Please see supplemental document for additional experimental procedure information.

RESOURCE AVAILABILITY

Lead contact

Further requests for reagents should be directed to and will be fulfilled by the corresponding author, Changyong Tang (tangchy23@mail.sysu.edu.cn).

Materials availability

All unique/stable reagents generated in this study are available from the lead contact with a completed materials transfer agreement.

Data and code availability

All data presented in this study are available in the supplemental file and can be obtained from the corresponding authors upon request.

ACKNOWLEDGMENTS

We thank Peijian Peng and Min Yang for helpful discussion and technical assistance. We also thank Professor Weibin Cai (Sun Yat-sen University) for kindly providing us with *PKM2*$^{fl/fl}$ mice. This research was supported by grants from the Science and Technology Plan Project of Guangzhou City 2023A04J1089 (C.T.)., National Key R&D Program of China grant 2022ZD02 14300 (C.T.), the National Natural Science Foundation of China grants 82471382 (C.T.), 82401413 (W.J.) and 32300804 (Y.Z.), and the GDAS' Project of Science and Technology Development grants 2022GDASZH-2022010110 (C.W.), 2022GDASZH-2022030603-01 (C.W.), and 2023GDASZH-2023030602 (C.W.).

AUTHOR CONTRIBUTIONS

Conceptualization, C.T., C.W., and Y.W.; methodology, P.H., W.J., F.Z., Z.L., and L.G.; investigation, P.H., W.J., and F.Z.; writing – original draft, P.H.; writing – review and editing, P.H. and C.T.; funding acquisition, C.T.; supervision, C.T.; project administration, C.T.

DECLARATION OF INTERESTS

The authors declare no competing interests.

SUPPLEMENTAL INFORMATION

Supplemental information can be found online at https://doi.org/10.1016/j.stemcr.2024.11.011.

Received: June 15, 2024
Revised: November 20, 2024
Accepted: November 21, 2024
Published: December 19, 2024

REFERENCES

Ahmed, K., Tunaru, S., and Offermanns, S. (2009). GPR109A, GPR109B and GPR81, a family of hydroxy-carboxylic acid receptors. Trends Pharmacol. Sci. *30*, 557–562.

Ben-Zeev, T., Shoenfeld, Y., and Hoffman, J.R. (2022). The Effect of Exercise on Neurogenesis in the Brain. Isr. Med. Assoc. J. *24*, 533–538.

Bergersen, L.H. (2015). Lactate transport and signaling in the brain: potential therapeutic targets and roles in body-brain interaction. J. Cerebr. Blood Flow Metabol. *35*, 176–185.

Bond, A.M., Ming, G.L., and Song, H. (2015). Adult Mammalian Neural Stem Cells and Neurogenesis: Five Decades Later. Cell Stem Cell *17*, 385–395.

Chen, D., Wei, L., Liu, Z.R., Yang, J.J., Gu, X., Wei, Z.Z., Liu, L.P., and Yu, S.P. (2018). Pyruvate Kinase M2 Increases Angiogenesis, Neurogenesis, and Functional Recovery Mediated by Upregulation of STAT3 and Focal Adhesion Kinase Activities After Ischemic Stroke in Adult Mice. Neurotherapeutics *15*, 770–784.

Chen, M., David, C.J., and Manley, J.L. (2012). Concentration-dependent control of pyruvate kinase M mutually exclusive splicing by hnRNP proteins. Nat. Struct. Mol. Biol. *19*, 346–354.

Deitmer, J.W., Theparambil, S.M., Ruminot, I., Noor, S.I., and Becker, H.M. (2019). Energy Dynamics in the Brain: Contributions of Astrocytes to Metabolism and pH Homeostasis. Front. Neurosci. *13*, 1301.

Elizondo-Vega, R., and García-Robles, M.A. (2017). Molecular Characteristics, Regulation, and Function of Monocarboxylate Transporters. Adv. Neurobiol. *16*, 255–267.

Epp, J.R., Silva Mera, R., Köhler, S., Josselyn, S.A., and Frankland, P.W. (2016). Neurogenesis-mediated forgetting minimizes proactive interference. Nat. Commun. *7*, 10838.

Feng, Y., Li, X., Wang, J., Huang, X., Meng, L., and Huang, J. (2022). Pyruvate kinase M2 (PKM2) improve symptoms of post-ischemic stroke depression by activating VEGF to mediate the MAPK/ERK pathway. Brain Behav. *12*, e2450.

Ferreira, A.C., Sousa, N., Bessa, J.M., Sousa, J.C., and Marques, F. (2018). Metabolism and adult neurogenesis: Towards an understanding of the role of lipocalin-2 and iron-related oxidative stress. Neurosci. Biobehav. Rev. *95*, 73–84.

Folmes, C.D.L., Nelson, T.J., Martinez-Fernandez, A., Arrell, D.K., Lindor, J.Z., Dzeja, P.P., Ikeda, Y., Perez-Terzic, C., and Terzic, A. (2011). Somatic oxidative bioenergetics transitions into pluripotency-dependent glycolysis to facilitate nuclear reprogramming. Cell Metabol. *14*, 264–271.

Gonçalves, J.T., Schafer, S.T., and Gage, F.H. (2016). Adult Neurogenesis in the Hippocampus: From Stem Cells to Behavior. Cell *167*, 897–914.

Guo, W., Patzlaff, N.E., Jobe, E.M., and Zhao, X. (2012). Isolation of multipotent neural stem or progenitor cells from both the dentate gyrus and subventricular zone of a single adult mouse. Nat. Protoc. *7*, 2005–2012.

Jin, E.S., Lee, M.H., Murphy, R.E., and Malloy, C.R. (2018). Pentose phosphate pathway activity parallels lipogenesis but not antioxidant processes in rat liver. Am. J. Physiol. Endocrinol. Metab. *314*. E543-e551.

Kennedy, L., Glesaaen, E.R., Palibrk, V., Pannone, M., Wang, W., Al-Jabri, A., Suganthan, R., Meyer, N., Austbø, M.L., Lin, X., et al. (2022). Lactate receptor HCAR1 regulates neurogenesis and microglia activation after neonatal hypoxia-ischemia. Elife *11*, e76451.

Lambertus, M., Øverberg, L.T., Andersson, K.A., Hjelden, M.S., Hadzic, A., Haugen, Ø.P., Storm-Mathisen, J., Bergersen, L.H., Geiseler, S., and Morland, C. (2021). L-lactate induces neurogenesis in the mouse ventricular-subventricular zone via the lactate receptor HCA1. Acta Physiol. *231*, e13587.

Lauritzen, K.H., Morland, C., Puchades, M., Holm-Hansen, S., Hagelin, E.M., Lauritzen, F., Attramadal, H., Storm-Mathisen, J., Gjedde, A., and Bergersen, L.H. (2014). Lactate receptor sites link neurotransmission, neurovascular coupling, and brain energy metabolism. Cerebr. Cortex *24*, 2784–2795.

Lev-Vachnish, Y., Cadury, S., Rotter-Maskowitz, A., Feldman, N., Roichman, A., Illouz, T., Varvak, A., Nicola, R., Madar, R., and Okun, E. (2019). L-Lactate Promotes Adult Hippocampal Neurogenesis. Front. Neurosci. *13*, 403.

Li, J., Zhang, B., Jia, W., Yang, M., Zhang, Y., Zhang, J., Li, L., Jin, T., Wang, Z., Tao, J., et al. (2021). Activation of Adenosine Monophosphate-Activated Protein Kinase Drives the Aerobic Glycolysis in Hippocampus for Delaying Cognitive Decline Following Electroacupuncture Treatment in APP/PS1 Mice. Front. Cell. Neurosci. *15*, 774569.

Liu, W., Zhuo, P., Li, L., Jin, H., Lin, B., Zhang, Y., Liang, S., Wu, J., Huang, J., Wang, Z., et al. (2017). Activation of brain glucose metabolism ameliorating cognitive impairment in APP/PS1 transgenic mice by electroacupuncture. Free Radic. Biol. Med. *112*, 174–190.

Liu, Z., Le, Y., Chen, H., Zhu, J., and Lu, D. (2021). Role of PKM2-Mediated Immunometabolic Reprogramming on Development of Cytokine Storm. Front. Immunol. *12*, 748573.

Mazurek, S., Boschek, C.B., Hugo, F., and Eigenbrodt, E. (2005). Pyruvate kinase type M2 and its role in tumor growth and spreading. Semin. Cancer Biol. *15*, 300–308.

Morland, C., Andersson, K.A., Haugen, Ø.P., Hadzic, A., Kleppa, L., Gille, A., Rinholm, J.E., Palibrk, V., Diget, E.H., Kennedy, L.H., et al. (2017). Exercise induces cerebral VEGF and angiogenesis via the lactate receptor HCAR1. Nat. Commun. *8*, 15557.

Nayak, M.K., Ghatge, M., Flora, G.D., Dhanesha, N., Jain, M., Markan, K.R., Potthoff, M.J., Lentz, S.R., and Chauhan, A.K. (2021). The metabolic enzyme pyruvate kinase M2 regulates platelet function and arterial thrombosis. Blood *137*, 1658–1668.

Palsson-McDermott, E.M., Curtis, A.M., Goel, G., Lauterbach, M.A.R., Sheedy, F.J., Gleeson, L.E., van den Bosch, M.W.M., Quinn, S.R., Domingo-Fernandez, R., Johnston, D.G.W., et al. (2015). Pyruvate kinase M2 regulates Hif-1α activity and IL-1β induction and is a critical determinant of the warburg effect in LPS-activated macrophages. Cell Metabol. *21*, 65–80.

Pan, R.Y., He, L., Zhang, J., Liu, X., Liao, Y., Gao, J., Liao, Y., Yan, Y., Li, Q., Zhou, X., et al. (2022). Positive feedback regulation of microglial glucose metabolism by histone H4 lysine 12 lactylation in Alzheimer's disease. Cell Metabol. *34*, 634–648.e6.

Quistorff, B., Secher, N.H., and Van Lieshout, J.J. (2008). Lactate fuels the human brain during exercise. Faseb. J. *22*, 3443–3449.

Romero-Ramírez, L., García-Rama, C., Wu, S., and Mey, J. (2022). Bile acids attenuate PKM2 pathway activation in proinflammatory microglia. Sci. Rep. *12*, 1459.

Sharma, D., Singh, M., and Rani, R. (2022). Role of LDH in tumor glycolysis: Regulation of LDHA by small molecules for cancer therapeutics. Semin. Cancer Biol. *87*, 184–195.

So, J.H., Huang, C., Ge, M., Cai, G., Zhang, L., Lu, Y., and Mu, Y. (2017). Intense Exercise Promotes Adult Hippocampal Neurogenesis But Not Spatial Discrimination. Front. Cell. Neurosci. *11*, 13.

Tronel, S., Belnoue, L., Grosjean, N., Revest, J.M., Piazza, P.V., Koehl, M., and Abrous, D.N. (2012). Adult-born neurons are necessary for extended contextual discrimination. Hippocampus *22*, 292–298.

Valvona, C.J., Fillmore, H.L., Nunn, P.B., and Pilkington, G.J. (2016). The Regulation and Function of Lactate Dehydrogenase A: Therapeutic Potential in Brain Tumor. Brain Pathol. *26*, 3–17.

van Praag, H., Shubert, T., Zhao, C., and Gage, F.H. (2005). Exercise enhances learning and hippocampal neurogenesis in aged mice. J. Neurosci. *25*, 8680–8685.

Vorhees, C.V., and Williams, M.T. (2006). Morris water maze: procedures for assessing spatial and related forms of learning and memory. Nat. Protoc. *1*, 848–858.

Wu, B., Liang, Z., Lan, H., Teng, X., and Wang, C. (2024). The role of PKM2 in cancer progression and its structural and biological basis. J. Physiol. Biochem., 1–15.

Xu, S.N., Wang, T.S., Li, X., and Wang, Y.P. (2016). SIRT2 activates G6PD to enhance NADPH production and promote leukaemia cell proliferation. Sci. Rep. *6*, 32734.

Zhao, X., and van Praag, H. (2020). Steps towards standardized quantification of adult neurogenesis. Nat. Commun. *11*, 4275.

Zhou, J., Liu, T., Guo, H., Cui, H., Li, P., Feng, D., Hu, E., Huang, Q., Yang, A., Zhou, J., et al. (2018). Lactate potentiates angiogenesis and neurogenesis in experimental intracerebral hemorrhage. Exp. Mol. Med. *50*, 1–12.

Zhu, S., Guo, Y., Zhang, X., Liu, H., Yin, M., Chen, X., and Peng, C. (2021). Pyruvate kinase M2 (PKM2) in cancer and cancer therapeutics. Cancer Lett. *503*, 240–248.